

## TABLE OF CONTENTS

### **Simplified Preparation of $\text{REBa}_2\text{Cu}_3\text{O}_{7-x}$ Via the Acetate Method**

J. McHale, G.H. Myer, R.E. Salomon

### **Elastic Constants and Microcracks in $\text{YBa}_2\text{Cu}_3\text{O}_7$**

Y. Shindo, H. Ledbetter, H. Nozaki

### **Morphological and Structural Properties of High Quality YBCO Thin Films**

A. Cassinese, A. Di Chiara, F. Mileto Granozio, S. Saiello, U. Scotti di Uccio, M. Valentino

### **Strontium Aluminum Tantalum Oxide and Strontium Aluminum Niobium Oxide as Potential Substrates for HTSC Thin Films**

R. Guo, A.S. Bhalla, J. Sheen, F.W. Ainger, S. Erdei, E.C. Subbarao, L.E. Cross

### **Chemistry, Microstructure, and Electrical Properties at Interfaces Between Thin Films of Cobalt and Alpha (6H) Silicon Carbide (0001)**

L.M. Porter, R.F. Davis, J.S. Bow, M.J. Kim, R.W. Carpenter

### **Thermoelectric Generators Made of $\text{FeSi}_2$ and HMS: Fabrication and Measurement**

E. Groß, M. Riffel, U. Stöhrer

### **Optical Measurement of the Elastic Moduli and Thermal Diffusivity of a C-N Film**

Y. Yang, K.A. Nelson, F. Adibi

### **Crystal Orientation and Near-Interface Structure of Chemically Vapor Deposited $\text{MoS}_2$ Films**

W.Y. Lee, K.L. More

### **Laser-Induced Microstructural Changes and Decomposition of Aluminum Nitride**

S. Cao, A.J. Pedraza, L.F. Allard

### **Zirconia-Mullite Ceramics Made from Composite Particles Coated with Amorphous Phase: I. Effect of Zirconia Addition**

J.-J. Shyu, Y.-C. Chen

### **Synthesis and Characterization of Sol-Gel Derived Lanthanum Hexaluminate Powders and Films**

M.K. Cinibulk

### **Submicrometer Zinc Oxide Particles: Elaboration in Polyol Medium and Morphological Characteristics**

D. Jézéquel, J. Guenot, N. Jouini, F. Fiévet

### **Factors Influencing the Formation of Hollow Ceramic Microspheres by Water Extraction of Colloidal Droplets**

J.G. Liu, D.L. Wilcox, Sr.

### **Effect of Machining Residual Stresses on the Repetitive Impact Behavior of Silicon Nitride**

S. Srinivasan, P.J. Blau, J.L. Bjerke

### **Determining the Mechanical Properties of Small Volumes of Material from Sub-Micrometer Spherical Indentations**

J.S. Field, M.V. Swain

### **Mechanical Properties of a 20 vol%SiC Whisker-Reinforced Ytria-Stabilized, Tetragonal Zirconia Composite at Elevated Temperatures**

S.E. Dougherty, T.G. Nieh, J. Wadsworth, Y. Akimune

### **Microprobe Raman Spectroscopy of TiN Coatings Oxidized by Solar Beam Heat Treatment**

M. Franck, J.-P. Celis, J.R. Roos

### **B2 and B32 Ordering Transformations of Equiatomic bcc Alloys with Ballistic and Thermal Atom Movements**

L.B. Hong, L. Anthony, B. Fultz

### **Partial Melting and Segregation Behavior in a Superplastic $\text{Si}_3\text{N}_4/\text{Al-Mg}$ Alloy Composite**

J. Koike, M. Mabuchi, K. Higashi

### **The Structure and Property Characteristics of Amorphous/Nanocrystalline Silicon Produced by Ball Milling**

T.D. Shen, C.C. Koch, T.L. McCormick, R.J. Nemanich, J.Y. Huang, J.G. Huang

### **An Experimental Study of the Temperature and Stoichiometry Dependence of Diamond Growth in Low Pressure Flat Flames**

J.S. Kim, M.A. Cappelli

### **Formation of Highly Oriented Diamond Film on Carburized (100) Si Substrate**

H. Maeda, M. Irie, T. Hino, K. Kusakabe, S. Morooka

### **Diamond Nucleation on Unscratched Silicon Substrates Coated with Various Nondiamond Carbon Films by Microwave Plasma-Enhanced Chemical Vapor Deposition**

Z. Feng, M.A. Brewer, K. Komvopoulos, I.G. Brown, D.B. Bogy

### **Shock Compression of Graphite Materials Bearing Different Microtextures and Their Relations to Diamond Transition**

H. Hirai, T. Ohwada, K. Kondo

### **The Behavior of Screw Dislocations Dynamically Emitted from the Tip of a Surface Crack during Loading and Unloading**

C.C. Huang, C.C. Yu, S. Lee

### **Improved Wear Properties of High Energy Ion-Implanted Polycarbonate**

G.R. Rao, E.H. Lee, R. Bhattacharya, A.W. McCormick

### **Luminescence of Polymer Electrolytes Containing Europium (III)**

L.D. Carlos, M. Assunção, L. Alcácer

### **Investigation of the Effect of Host Composition on the Photoluminescent Properties of $\text{Sr}_x\text{Ba}_{1-x}\text{S}$ Doped with Eu and Sm**

D.T. Brower, I.K. Lloyd

### **Growth Kinetics, Phase Transitions and Cracking in Cholesterol Gallstones**

S. Kumar, S.J. Burns, T.N. Blanton

## ABSTRACTS

**Simplified Preparation of REBa<sub>2</sub>Cu<sub>3</sub>O<sub>7-x</sub> Via the Acetate Method**

J. McHale, G.H. Myer, R.E. Salomon  
(Temple University)

High quality bulk REBa<sub>2</sub>Cu<sub>3</sub>O<sub>7-x</sub> (RE = Y, Eu, Gd, Nd, La) was synthesized by a solution method. Stoichiometric amounts of yttrium, barium, and copper acetates were dissolved in glacial acetic acid. The acid was boiled away leaving a glassy acetate precursor. This precursor has shown amorphous scattering in XRD, a phenomenon consistent with atomic level mixing of reactants. The glassy precursor was subsequently heat treated with a 5°C/min ramp to 900°C and a 2 h soak at 900°C in air. The final product was obtained after heat treatment under oxygen at 550°C with slow cooling to room temperature. Final products were analyzed by XRD, SEM, and four probe dc-resistivity measurements and show phase pure, orthorhombic material with a superconducting transition temperature for YBa<sub>2</sub>Cu<sub>3</sub>O<sub>7-x</sub> of 92 K. The mechanism of both precursor and product formation was examined through substitution studies and XRD. It was found that a combination of a rare earth acetate, barium acetate, and acetic acid was necessary for the formation of an amorphous precursor.

Order No.: JA501-001

© 1995 MRS

**Elastic Constants and Microcracks in YBa<sub>2</sub>Cu<sub>3</sub>O<sub>7</sub>**

Y. Shindo\*, H. Ledbetter\*, H. Nozaki\*  
(\*Tohoku University, \*National Institute of Standards and Technology, \*Tokyo National College of Technology)

We analyze theoretically the effect of microcracks and voids on the apparent elastic constants of polycrystalline YBa<sub>2</sub>Cu<sub>3</sub>O<sub>7</sub>. Using measurements by Holcomb and Mayo, we calculate crack density and crack aspect ratio. We obtain reasonable intrinsic elastic constants. For the bulk modulus, for example, we predict values close to those obtained by neutron-diffraction studies: 123 GPa for a polycrystal and 122 for a monocrystal.

Order No.: JA501-002

© 1995 MRS

**Morphological and Structural Properties of High Quality YBCO Thin Films**

A. Cassinese, A. Di Chiara, F. Mileto Granozio, S. Saiello, U. Scotti di Uccio, M. Valentino  
(Università Federico II di Napoli)

High quality YBCO thin films have been grown by Inverted Cylindrical Magnetron Sputtering (ICMS) on LaAlO<sub>3</sub> (100), SrTiO<sub>3</sub> (100), SrTiO<sub>3</sub> (110) and MgO (100) substrates. Transition temperatures of c-axis films exceed 90 K and transition widths are within 1 K. Critical currents range up to 5x10<sup>6</sup> A/cm<sup>2</sup> at 77 K. Structural and morphological features, respectively analyzed by x-ray diffraction and scanning electron microscopy, are found to be strongly dependent on film orientation and deposition temperature. In order to understand such dependence a simple interpretation is proposed in terms of Gibbs energies and growth dynamics of nucleation process.

Order No.: JA501-003

© 1995 MRS

**Strontium Aluminum Tantalum Oxide and Strontium Aluminum Niobium Oxide as Potential Substrates for HTSC Thin Films**

R. Guo, A.S. Bhalla, J. Sheen, F.W. Ainger, S. Erdei, E.C. Subbarao, L.E. Cross  
(The Pennsylvania State University)

Single crystal fibers of A(B<sub>1/2</sub>B<sub>2/2</sub>)O<sub>3</sub> perovskites type with compositions Sr(Al<sub>1/2</sub>Ta<sub>1/2</sub>)O<sub>3</sub> (SAT) and Sr(Al<sub>1/2</sub>Nb<sub>1/2</sub>)O<sub>3</sub> (SAN) were grown successfully for the first time, using a laser heated pedestal growth (LHPG) technique. Their crystallographic structures were found to be simple cubic perovskite with lattice parameters a = 3.8952 Å (SAT) and a = 3.8995 Å (SAN) that are close lattice matches to the YBCO superconductors. No structural phase transitions or twins have been found, and the average coefficients of the thermal expansion match well with the YBCO superconductor materials. We report that SAT is one of the most promising substrates to date for the epitaxial growth of HTSC thin films suitable for microwave device applications as it has low dielectric constants (κ~11-12, at 100Hz-10GHz and

300 K) and low dielectric loss (~4x10<sup>-5</sup> at 10kHz and 80 K), together with lattice parameter matching, thermal expansion matching and chemical compatibility with the high T<sub>C</sub> superconductors (YBCO).

Order No.: JA501-004

© 1995 MRS

**Chemistry, Microstructure, and Electrical Properties at Interfaces Between Thin Films of Cobalt and Alpha (6H) Silicon Carbide (0001)**

L.M. Porter\*, R.F. Davis\*, J.S. Bow\*, M.J. Kim\*, R.W. Carpenter\*  
(\*North Carolina State University, \*Arizona State University)

Thin films (4-1000 Å) of Co were deposited onto n-type 6H-SiC (0001) wafers by UHV electron beam evaporation. The chemistry, microstructure, and electrical properties were determined using x-ray photoelectron spectroscopy, high resolution transmission electron microscopy, and I-V and C-V measurements, respectively. The as-deposited contacts exhibited excellent rectifying behavior with low ideality factors and leakage currents of n<1.06 and 2.0x10<sup>-8</sup> A/cm<sup>2</sup> at -10 V, respectively. During annealing at 1000°C for 2 min., significant reaction occurred resulting in the formation CoSi and graphite. These annealed contacts exhibited ohmic-like character, which is believed to be due to defects created in the interface region.

Order No.: JA501-005

© 1995 MRS

**Thermoelectric Generators Made of FeSi<sub>2</sub> and HMS: Fabrication and Measurement**

E. Groß, M. Riffel, U. Stöhrer  
(Universität Karlsruhe)

Single couple thermoelectric generators consisting of n-type FeSi<sub>2</sub> and p-type higher manganese silicide were developed and characterized. The leg and the bridge materials were prepared by powder metallurgical method. Using the Peltier effect, the transport properties were measured over the whole working temperature range. Electrical contacts suitable for the hot side could be obtained by conventional vacuum soldering and those for the cold side by ultrasonic soldering. The measured efficiency was in excellent agreement with the calculated values derived from the leg and contact properties.

Order No.: JA501-006

© 1995 MRS

**Optical Measurement of the Elastic Moduli and Thermal Diffusivity of a C-N Film**

Y. Yang\*, K.A. Nelson\*, F. Adibi\*  
(\*Massachusetts Institute of Technology, \*Northwestern University)

The elastic properties of a carbon nitride (CN<sub>x</sub>) film adhered to a silicon substrate were characterized through impulsive stimulated thermal scattering (ISTS). The lowest-order pseudo-Rayleigh acoustic mode of the film was excited and monitored optically. From the measured acoustic phase velocities, the elastic moduli of the film were determined. The ISTS technique also permits measurement of the CN<sub>x</sub> thermal diffusivity. The noninvasive optical measurements described can provide a useful guide to refinements in thin film fabrication procedures and for optimization of mechanical and thermal transport properties.

Order No.: JA501-007

© 1995 MRS

**Crystal Orientation and Near-Interface Structure of Chemically Vapor Deposited MoS<sub>2</sub> Films**

W.Y. Lee, K.L. More  
(Oak Ridge National Laboratory)

Crystalline MoS<sub>2</sub> films were deposited on Si and graphite substrates using MoF<sub>6</sub> and H<sub>2</sub>S as precursors. The crystal orientation and near-interface structure of the MoS<sub>2</sub> films were studied using transmission electron microscopy. In general, the preferred orientation of the (002) basal planes of the MoS<sub>2</sub> films with respect to the substrate surface changed from parallel to perpendicular with increased deposition temperature from 330 to 430°C. At 430°C, the basal planes were primarily oriented perpendicular to the Si substrate, except for the presence of a 5 nm interface region in which the basal planes were oriented in the parallel direction. The formation of this transitional region was also observed on the graphite substrate.

Order No.: JA501-008

© 1995 MRS

### Laser-Induced Microstructural Changes and Decomposition of Aluminum Nitride

S. Cao\*, A.J. Pedraza\*, L.F. Allard\*

(\*University of Tennessee, \*Oak Ridge National Laboratory)

The microstructural changes induced by pulsed laser irradiation in the surface layer of AlN and the initial stage of electroless copper deposition in laser processed specimens have been investigated using transmission electron microscopy (TEM). It was found that a dislocation microstructure is generated by laser processing at laser energy densities of 1.5 J/cm<sup>2</sup> or higher. A very sharp change in the dislocation microstructure was seen at a depth of 0.2 to 0.3 μm from the free surface. The dislocations Burgers vector is  $\langle 100 \rangle$  and the slip plane is {001}, in agreement with previous reports.

AlN was melted and resolidified homo-epitactically from the solid substrate forming a mosaic microstructure with very fine cells having a misorientation of up to 15°. Patches of metallic aluminum were found at the surface of all the specimens irradiated at a laser energy density of 1.5 J/cm<sup>2</sup> or higher. Very fine particles of AlN, 20 to 50 nm in diameter, were randomly distributed inside the patches. Immersion of these specimens in an electroless copper bath showed that the electroless solution preferentially etched away aluminum at the Al-AlN interface. At the same time copper islands were deposited in cavities left by AlN particles as well as at the interface with the underlying substrate. These regions are the seeds for further electroless deposition. The TEM observations of laser-induced microstructural changes reported in this paper help to further unravel the mechanisms of adhesion enhancement and surface activation by pulsed laser irradiation.

Order No.: JA501-009

© 1995 MRS

### Zirconia-Mullite Ceramics Made from Composite Particles Coated with Amorphous Phase: I. Effect of Zirconia Addition

J.-J. Shyu, Y.-C. Chen

(Tatung Institute of Technology)

Mullite-based ceramics added with 0–20 vol% stabilized zirconia have been prepared by alumina/zirconia particles coated with an amorphous silica layer. All samples can be densified through the viscous flow of the amorphous silica layer in the typical temperature range of 1100°–1310°C. For the ZrO<sub>2</sub>-free mullite ceramics, the viscous densification kinetics is inhibited by increasing the content of the alumina inclusion particles and by crystallization of the amorphous silica layer. However, for the zirconia-mullite ceramics, the addition of the zirconia inclusion particles accelerates the viscous densification kinetics. Mullitization kinetics is also enhanced by the addition of zirconia. As the sintering temperature is high, a porous, duplex microstructure is observed in samples with or without zirconia. Zirconia addition enhances the development of this microstructure. As the sintering temperature and/or zirconia content is increased, ZrO<sub>2</sub> particles tend to coarsen, resulting in a decreased tetragonal to monoclinic ratio. Fracture toughness K<sub>1c</sub> increases with the zirconia content. Mullite-20 vol% ZrO<sub>2</sub> composite sintered at 1600°C has a K<sub>1c</sub> of 3.8 MPa·m<sup>1/2</sup>.

Order No.: JA501-010

© 1995 MRS

### Synthesis and Characterization of Sol-Gel Derived Lanthanum Hexaluminate Powders and Films

M.K. Cinibulk

(Wright Laboratory)

Powders and thin films of high-yield lanthanum hexaluminate (LaAl<sub>11</sub>O<sub>18</sub>) were prepared by a sol-gel route and compared with yields obtained by conventional hot-pressing of oxide powders. X-ray diffraction and transmission electron microscopy (TEM) were used to characterize powders and thin films deposited on TEM grids. While the solid-state kinetics of formation of LaAl<sub>11</sub>O<sub>18</sub> are known to be extremely sluggish, the yield of LaAl<sub>11</sub>O<sub>18</sub> formed by the sol-gel route was much higher than that obtained by processing under similar conditions by solid-state reaction of elemental oxides. The development of a very fine grained microstructure at 1200°C and a coarser, much more mature microstructure at 1450°C, with strong texturing of the magnetoplumbite phase, was observed by TEM. Isolated grains of LaAlO<sub>3</sub> were present in all powders and films. Trace impurities, introduced most likely as impurities in the initial alumina sol, appear to have seg-

regated to both the grain boundaries and to the external surfaces of grains in as-prepared films.

Order No.: JA501-011

© 1995 MRS

### Submicrometer Zinc Oxide Particles: Elaboration in Polyol Medium and Morphological Characteristics

D. Jézéquel, J. Guenot, N. Jouini, F. Fiévet

(Université Paris 7-Denis Diderot)

A novel and easy route for preparing submicrometer particles of zinc oxide, involving hydrolysis of zinc salt in a polyol medium, is proposed. Zinc acetate dihydrate and diethyleneglycol appear to be the best candidates for obtaining a high yield of particles with well-defined morphological characteristics. Monodisperse spherical particles in the submicrometer range (0.2–0.4 μm) have been obtained for a salt concentration less than 0.1 mol l<sup>-1</sup>. The particle size depends mainly on the heating rate. The particles are microporous (surface area: 80 m<sup>2</sup> g<sup>-1</sup>) and are formed by aggregation of small crystallites (10 nm). Calcination at moderate temperature drastically reduces this porosity without significant interparticle sintering. At higher concentration, no aggregation occurs and tiny single crystallite particles are obtained.

Order No.: JA501-012

© 1995 MRS

### Factors Influencing the Formation of Hollow Ceramic Microspheres by Water Extraction of Colloidal Droplets

J.G. Liu, D.L. Wilcox, Sr.

(University of Illinois)

Hollow ceramic microspheres of Al<sub>2</sub>O<sub>3</sub>, SiO<sub>2</sub>, and mullite have been prepared by the combination of an emulsion technique with a water extraction sol-gel method. Concentration of sol, initial droplet size, and water extraction rate of the system are found to be the important process parameters controlling the size and wall thickness of the hollow microspheres, and their influences are shown. A model that correlates the morphology of microspheres to concentration and water extraction rate is proposed and is in good agreement with the experimental observations. The capability and limitation of this process for forming hollow microspheres are demonstrated. It was shown that hollow microspheres with sizes greater than 5 μm could be readily prepared, while a limitation was met for sizes less than 1 μm, in which case solid microspheres were normally formed.

Order No.: JA501-013

© 1995 MRS

### Effect of Machining Residual Stresses on the Repetitive Impact Behavior of Silicon Nitride

S. Srinivasan\*, P.J. Blau\*, J.L. Bjerke\*

(\*Oak Ridge National Laboratory, \*Caterpillar Technical Center)

Silicon nitride is a candidate valve material for internal combustion engines. Its low density and attractive mechanical properties relative to conventional metallic alloys portend significant improvements in valve performance. The production of valves involves a significant amount of machining, especially grinding. Grinding of ceramic materials may result in surface and sub-surface damage in the form of fracture or residual stresses which may affect impact behavior, and consequently, the behavior of silicon nitride ceramic materials as valves. The effects of residual stresses due to grinding on the impact wear behavior of one silicon nitride composition ground under various conditions has been investigated.

Order No.: JA501-014

© 1995 MRS

### Determining the Mechanical Properties of Small Volumes of Material from Sub-Micrometer Spherical Indentations

J.S. Field\*, M.V. Swain\*\*

(\*University of Sydney, \*\*CSIRO Division of Applied Physics)

The stress/strain behavior of bulk material is usually investigated in uniaxial tension or compression; however, these methods are not generally available for very small volumes of material. Sub-micrometer indentation using a spherical indenter has the potential for filling this gap with, possibly, access to hardness and elastic modulus profiles, representative stress/strain curves and the strain hardening index. The proposed techniques are based on principles well established in hardness testing using spherical indenters but not previously applied to

depth sensing instruments capable of measurements on a sub-micrometer scale. These approaches are now adapted to the analysis of data obtained by stepwise indentation with partial unloading; a technique which facilitates separation of the elastic and plastic components of indentation at each step and able to take account of the usually ignored phenomena of "piling up" and "sinking in."

Order No.: JA501-015

© 1995 MRS

#### Mechanical Properties of a 20 vol%SiC Whisker-Reinforced Yttria-Stabilized, Tetragonal Zirconia Composite at Elevated Temperatures

S.E. Dougherty\*, T.G. Nieh\*, J. Wadsworth\*, Y. Akimune\*  
(\*Lawrence Livermore National Laboratory, \*Nissan Motor Co., Ltd.)

The high-temperature deformation behavior of a SiC whisker-reinforced, yttria-stabilized, tetragonal zirconia polycrystalline composite containing 20 vol.% SiC whiskers (SiC/Y-TZP) has been investigated. Tensile tests were performed in vacuum at temperatures from 1450°C to 1650°C and at strain rates from  $10^{-3}$  to  $10^{-5}$  s $^{-1}$ . The material exhibits useful high temperature engineering properties (e.g., ~100 MPa and 16% elongation at T = 1550°C and at a strain rate of  $\sim 10^{-4}$  s $^{-1}$ ). The stress exponent was determined to be  $n \approx 2$ . Scanning electron microscopy was used to characterize the grain size and morphology of the composites, both before and after deformation. The grain size in the composite was initially fine, but coarsened at the test temperatures; both dynamic and static grain growth were observed. The morphology of ceramic reinforcements appears to affect strongly the plastic deformation properties of Y-TZP. A comparison is made between the properties of monolithic Y-TZP, 20 wt.% Al $_2$ O $_3$  particulate-reinforced Y-TZP (Al $_2$ O $_3$ /Y-TZP), and SiC/Y-TZP composites.

Order No.: JA501-016

© 1995 MRS

#### Microprobe Raman Spectroscopy of TiN Coatings Oxidized by Solar Beam Heat Treatment

M. Franck, J-P. Celis, J.R. Roos  
(Katholieke Universiteit Leuven)

Physical vapor deposited TiN coatings oxidized by solar beam heat treatment in air were examined by microprobe Raman spectroscopy. The Raman spectra of TiN treated at 400°C indicated incipient oxidation by the presence of anatase TiO $_2$  and additionally showed a broad band feature around the forbidden TiN vibrational mode. Inhomogeneous mixtures of rutile TiO $_2$  and small amounts of anatase polymorph (<10%) were detected for the treatments at 600°C only during the initial stage of oxidation. Prolonged treatment at 600°C resulted in a complete anatase-to-rutile conversion. Rutile was identified as the single product of oxidation of the TiN samples treated at 800°C. Peak analysis of the rutile spectra revealed no substantial spectral shifts, demonstrating an oxide growth of nearly stoichiometric rutile with an estimated composition in the range of TiO $_{2\pm 0.02}$ . The Raman scattered light intensity could be correlated with the rutile layer thickness.

Order No.: JA501-017

© 1995 MRS

#### B2 and B32 Ordering Transformations of Equiatomic bcc Alloys with Ballistic and Thermal Atom Movements

L.B. Hong, L. Anthony, B. Fultz  
(California Institute of Technology)

We used Monte Carlo simulations to study the kinetics and steady states of B2 and B32 ordering in an equiatomic binary bcc alloy having both thermal and ballistic atom movements. Atom movements occurred by a vacancy mechanism, where first-neighbor atoms exchanged sites with the vacancy. In the thermodynamic case, where this jump probability was set by a Boltzmann factor alone, we found the formation of large amounts of transient B2 (B32) during disorder  $\rightarrow$  B32 (B2) order transformations. The transient order developed in distinct regions, but vanished completely when equilibrium was attained. Ballistic jumps were included as random interchanges of the vacancy with one of its neighboring atoms. Even with small fractions of ballistic jumps, there were large changes in the transient states and steady states of order in the alloy. A kinetic explanation is proposed, in which the presence of ballistic jumps contributed a greater amount of internal energy to the B2 phase than to the B32 phase when there was a strong asymmetry in the second-nearest neighbor pair potentials

( $V_{AA2} \neq V_{BB2}$ ). A two-phase coexistence in the steady state was explained by fluctuations in the local density of ballistic jumps.

Order No.: JA501-018

© 1995 MRS

#### Partial Melting and Segregation Behavior in a Superplastic Si $_3$ N $_4$ /Al-Mg Alloy Composite

J. Koike\*, M. Mabuchi\*, K. Higashi\*

(\*Oregon State University, \*National Industrial Research Institute of Nagoya, #University of Osaka Prefecture)

Al-Mg alloy (5052) composite reinforced with particulate Si $_3$ N $_4$  particulates was investigated by transmission electron microscopy and electron energy loss spectroscopy. Partial melting was observed at matrix/reinforcements interfaces and matrix grain boundaries at a temperature near an optimum superplastic temperature. Segregation of solute elements (Mg and Si) was observed at the interfaces and grain boundaries. Both partial melting and solute segregation were found to depend on grain boundaries. The obtained results were explained by a decrease of the solidus temperature due to segregation whose extent depends on the type of the grain boundary structure.

Order No.: JA501-019

© 1995 MRS

#### The Structure and Property Characteristics of Amorphous/Nanocrystalline Silicon Produced by Ball Milling

T.D. Shen\*, C.C. Koch\*, T.L. McCormick\*, R.J. Nemanich\*, J.Y. Huang\*, J.G. Huang\*

(\*North Carolina State University, \*Academia Sinica)

The structural transformation of polycrystalline Si induced by high energy ball milling has been studied. The structure and property characteristics of the milled powder have been investigated by x-ray diffraction, scanning electron microscopy, high-resolution electron microscopy, differential scanning calorimetry, Raman scattering and infrared absorption spectroscopy. Two phase amorphous and nanocrystalline Si has been produced by ball milling of polycrystalline elemental Si. The nanocrystalline components contain some defects such as dislocations, twins and stacking faults which are typical of defects existing in conventional coarsened-grain polycrystalline materials. The volume fraction of amorphous Si is about 15% while the average size of nanocrystalline grains is about 8 nm. Amorphous elemental Si without combined oxygen can be obtained by ball milling. The distribution of amorphous Si and the size of nanocrystalline Si crystallites is not homogeneous in the milled powder. The amorphous Si formed is concentrated near the surface of milled particles while the grain size of nanocrystalline Si ranges from 3 to 20 nm. Structurally, the amorphous silicon component prepared by ball milling is similar to that obtained by ion implantation or chemical vapor deposition. The amorphous Si formed exhibits a crystallization temperature of about 660°C at a heating rate of 40 K/min and crystallization activation energy of about 268 kJ/mol. Two possible amorphization mechanisms, i.e., pressure-induced amorphization and crystallite-refinement-induced amorphization, are proposed for the amorphization of Si induced by ball milling.

Order No.: JA501-020

© 1995 MRS

#### An Experimental Study of the Temperature and Stoichiometry Dependence of Diamond Growth in Low Pressure Flat Flames

J.S. Kim, M.A. Cappelli

(Stanford University)

A study of the temperature and stoichiometry dependence of diamond synthesis in low pressure premixed acetylene-oxygen flames is presented. A specially designed low pressure flat flame operating at 40 Torr is employed to deposit diamond films uniformly over areas of at least 2 cm $^2$ . Under optimized conditions of substrate temperatures and flame equivalence ratios, high quality translucent diamond that is well faceted is synthesized exhibiting first-order Raman fullwidths (half maximum) of about 2.5 cm $^{-1}$ . Diamond growth rates under these optimum conditions are approximately 4  $\mu$ m/hour. The film growth rate is found to drop off substantially at high substrate temperatures, with little or no carbon deposited beyond a temperature of 1070°C. The growth behavior in response to changes in flame equivalence ratio and substrate temperature is discussed in terms of the possible role that

oxygen-containing species may have on surface chemistry. The results described here are also used to project a base cost for manufacturing diamond under these process conditions.

Order No.: JA501-021

© 1995 MRS

#### Formation of Highly Oriented Diamond Film on Carburized (100) Si Substrate

H. Maeda, M. Irie, T. Hino, K. Kusakabe, S. Morooka  
(Kyushu University)

Highly oriented diamond film was grown on a (100) Si substrate by a bias-enhanced microwave-plasma chemical vapor deposition. The Si surface was carburized at a faster rate by bias treatment than by carburization alone, but the initial carburization stage was indispensable. During the bias treatment, the flat surface was changed to a textured structure on the nanometer scale. The formation of this structure was required for the synthesis of a highly oriented diamond film. Diamond microcrystals formed subsequently were irregular and of a few to a few tens nanometers in size. Then they grew to oriented film in the following growth process.

Order No.: JA501-022

© 1995 MRS

#### Diamond Nucleation on Unscratched Silicon Substrates Coated with Various Nondiamond Carbon Films by Microwave Plasma-Enhanced Chemical Vapor Deposition

Z. Feng, M.A. Brewer, K. Komvopoulos, I.G. Brown, D.B. Bogy  
(University of California-Berkeley)

The efficacy of various nondiamond carbon films as precursors for diamond nucleation on unscratched silicon substrates was investigated with a conventional microwave plasma-enhanced chemical vapor deposition system. Silicon substrates were partially coated with various carbonaceous substances such as clusters consisting of a mixture of C<sub>60</sub> and C<sub>70</sub>, evaporated films of carbon and pure C<sub>70</sub>, and hard carbon produced by a vacuum arc deposition technique. For comparison, diamond nucleation on silicon substrates coated with submicrometer-sized diamond particles and uncoated smooth silicon surfaces was also examined under similar conditions. Except for evaporated carbon films, significantly higher diamond nucleation densities were obtained by subjecting the carbon-coated substrates to a low-temperature high-methane concentration hydrogen plasma treatment prior to diamond nucleation. The highest nucleation density (~3x10<sup>8</sup> cm<sup>-2</sup>) was obtained with hard carbon films. Scanning electron microscopy and Raman spectroscopy demonstrated that the diamond nucleation density increased with the film thickness and etching resistance. The higher diamond nucleation density obtained with the vacuum arc deposited carbon films may be attributed to the inherent high etching resistance, presumably resulting from the high content of sp<sup>3</sup> atomic bonds. Microscopy observations suggested that diamond nucleation in the presence of nondiamond carbon deposits resulted from carbon layers generated under the pretreatment conditions.

Order No.: JA501-023

© 1995 MRS

#### Shock Compression of Graphite Materials Bearing Different Microtextures and Their Relations to Diamond Transition

H. Hirai, T. Ohwada, K. Kondo  
(Tokyo Institute of Technology)

Microtexture dependence of starting graphite materials on diamond transition under shock compression was examined, taking account of two critical points: (1) For the starting materials, several different graphite materials, each of which possesses homogeneous microtexture throughout the material, were used. (2) In order to distinguish the effect of the microtexture from that of other external conditions, an advanced technique which made pressure-temperature condition common for the individual materials was developed. Four graphite materials, a glassy carbon, two types of carbon black, and artificial graphite foil were selected and characterized in detail by x-ray diffractometry, Raman spectroscopy, transmission electron microscopy (TEM), and electron energy loss spectroscopy (EELS) prior to the shock loading.

Shock compression was performed for the materials, changes in the microtexture and transformed products of the recovered samples were characterized by TEM and EELS, and the effect of the microtexture on the transition to diamond was also discussed.

Order No.: JA501-024

© 1995 MRS

#### The Behavior of Screw Dislocations Dynamically Emitted from the Tip of a Surface Crack during Loading and Unloading

C.C. Huang\*, C.C. Yu\*, S. Lee\*

(\*National Tsing Hua University, \*Chung Yuan Christian University)

The behavior of screw dislocations dynamically emitted from the tip of a surface crack during loading and unloading has been investigated using a discrete dislocation model. The critical stress intensity factor at the crack tip for dislocation emission is a function of friction stress, core radius of dislocation, and dislocations near the crack tip. During motion, the velocity of dislocation is assumed to be proportional to the effective shear stress to the third power. The effect of crack length and friction stress on dislocation distribution, plastic zone and dislocation-free zone during loading and unloading were examined.

Order No.: JA501-025

© 1995 MRS

#### Improved Wear Properties of High Energy Ion-Implanted Polycarbonate

G.R. Rao\*, E.H. Lee\*, R. Bhattacharya\*, A.W. McCormick\*

(\*Oak Ridge National Laboratory, \*UES, Inc.)

Polycarbonate (Lexan™) (PC) was implanted with 2 MeV B<sup>+</sup> and O<sup>+</sup> ions separately to fluences of 5x10<sup>17</sup>, 1x10<sup>18</sup> and 5x10<sup>18</sup> ions/m<sup>2</sup>, and characterized for changes in surface hardness and tribological properties. Results of tests showed that hardness values of all implanted specimens increased over those of the unirradiated material, and the O<sup>+</sup>-implantation was more effective in improving hardness for a given fluence than the B<sup>+</sup>-implantation. Reciprocating sliding wear tests using a nylon ball counterface yielded significant improvements for all implanted specimens except for the 5x10<sup>17</sup> ions/m<sup>2</sup> B<sup>+</sup>-implanted PC. Wear tests conducted with a 52100 steel ball yielded significant improvements for the highest fluence of 5x10<sup>18</sup> ions/m<sup>2</sup> for both ions, but not for the two lower fluences. The improvements in properties were related to Linear Energy Transfer (LET) mechanisms, where it was shown that the O<sup>+</sup> implantation caused greater ionization, thereby greater cross-linking at the surface corresponding to much better improvements in properties. The results were also compared with a previous study on PC using 200 keV B<sup>+</sup> ions. The present study indicates that high energy irradiation produces thicker, more cross-linked, harder, and more wear-resistant surfaces on polymers and thereby improves properties to a greater extent and more efficiently than lower energy ion implantation.

Order No.: JA501-026

© 1995 MRS

#### Luminescence of Polymer Electrolytes Containing Europium (III)

L.D. Carlos\*<sup>#</sup>, M. Assunção\*, L. Alcácer<sup>#</sup>

(\*Universidade de Évora, \*Universidade de Aveiro, <sup>#</sup>Instituto Superior Técnico)

The excitation and emission spectra of polymeric matrices—poly(ethylene oxide) (PEO) and poly(propylene oxide) (PPO)—containing different concentrations of EuBr<sub>3</sub> were recorded and most of the observed transitions identified. The Stark components of the <sup>7</sup>F<sub>0-4</sub>, <sup>5</sup>D<sub>0</sub> levels and the corresponding barycenters were calculated based on the emission lines assignment to the <sup>5</sup>D<sub>0,1</sub> → <sup>7</sup>F<sub>0-4</sub> transitions. The spectra were discussed in terms of a C<sub>2v</sub> local Eu<sup>3+</sup> coordination. The relative intensity of the <sup>5</sup>D<sub>0</sub> → <sup>7</sup>F<sub>2</sub> hypersensitive transition were related to the electrolytes morphological changes due to increasing europium concentration.

Order No.: JA501-027

© 1995 MRS

### Investigation of the Effect of Host Composition on the Photoluminescent Properties of $Sr_xBa_{1-x}S$ Doped with Eu and Sm

D.T. Brower\*, I.K. Lloyd\*

(\*Optex Communications Corporation, \*University of Maryland)

The effect of modifying the host composition on the photoluminescent properties of the IR stimuable phosphor system  $SrBaS:(Eu,Sm)$  was investigated. Spectral measurements (stimulated emission, fluorescent emission, excitation, and IR stimulation) were made on nine separate host compositions. The lattice constant, ionicity, and lattice strain affect Stark splitting of the rare earth excited states. While large shifts in the IR stimulated emission and fluorescence wavelengths were observed, no shift was observed for the peak excitation and IR stimulation wavelengths.

Order No.: JA501-028

© 1995 MRS

changes to anhydrous cholesterol; both forms are crystalline and exhibit polymorphic transformations. Synthetic stones grown from cholesterol were anhydrous and have a phase change at temperatures close to human body temperature. Optical microscopy established that this phase transformation cracks the spherulitic crystals perpendicular to the fast growth direction. Thermal expansion measurements demonstrate that upon heating, the low density, low temperature phase is transformed to a high density phase. This phase transformation and repeated cracking may prove to be useful in destroying natural gallstones, while suppressing this transformation and its associated cracking might aid in securing other solid cholesterol deposits within the human body.

Order No.: JA501-029

© 1995 MRS

### Growth Kinetics, Phase Transitions and Cracking in Cholesterol Gallstones

S. Kumar\*, S.J. Burns\*, T.N. Blanton\*

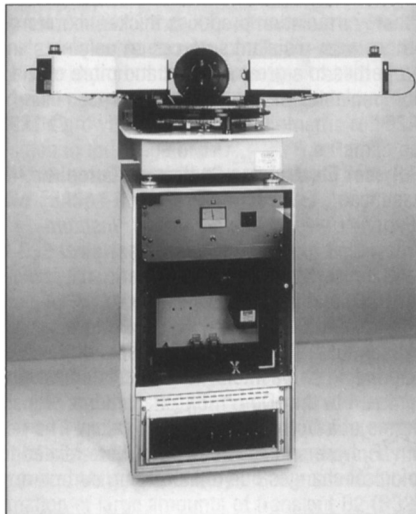
(\*University of Rochester, \*Eastman Kodak Company)

The growth kinetics of cholesterol gallstones have been studied by growing crystals from melted gallstones. The resulting microstructures are spherulitic, which are essentially the same as the structures seen in natural gallstones prior to melting. The cholesterol crystals, when observed in hot stage microscopy, emerge from a unique nucleation center growing radially in the [001] direction with constant rate. The DSC thermograph of a natural gallstone is initially similar to that of cholesterol monohydrate. Upon melting, cholesterol monohydrate

Please use the convenient postcard located in the back of the MRS Bulletin to order JMR reprints.

NEW

## GESP5 Integrated Optical Measurement Station



### Now measure...

- Variable Angle Spectroscopic Ellipsometry
- Reflection down to 6° angle of incidence
- Transmission up to 80° angle of incidence
- Refractometry for Brewster angle measurement of refractive index

...at one station.

### GESP5 unique features:

- Accurate control of angle of incidence
- High accuracy Spectroscopic Ellipsometry
- Wide spectral range
- Dual beam capability

### Powerful software package:

- Easy to use Windows™ based software interface for all measurements
- Wide variety of polynomial dispersion equations

Visit MRS Exhibit  
Booth No. U305

SOPRA S.A.  
26 Rue Pierre Joigneaux  
F-92270 Bois Colombes  
FRANCE  
TEL: 33-1-4781-0949  
FAX: 33-1-4242-2934

SOPRA GmbH  
Schuberstrasse 9-11  
DW 64572 Buettelborn 1  
GERMANY  
TEL: 49-61-52-5092  
FAX: 49-61-52-55201

SOPRA Inc  
P.O. Box 2619  
33 Nagog Park  
Acton, MA 01720  
TEL: 508 263-2520  
FAX: 508 263-2790

SEIKA Corp.  
Koraku International Building  
5-3, Koraku 1 Chome  
Bunkyo-Ku, Tokyo, 112  
TEL: 81-3-5684-7563  
FAX: 81-3-5684-7572

**SOPRA**

Circle No. 49 on Reader Service Card.